Autoimmune B-cell lymphopenia after successful adoptive therapy with telomerase-specific T lymphocytes

*Stefano Ugel,[1,2] *Elisa Scarselli,[3] Manuela Iezzi,[4] Carmela Mennuni,[3] Tania Pannellini,[4] Francesco Calvaruso,[3] Barbara Cipriani,[3] Raffaele De Palma,[5] Lucia Ricci-Vitiani,[6] Elisa Peranzoni,[1,7] Piero Musiani,[4] Paola Zanovello,[1,7] and Vincenzo Bronte[7]

[1]Department of Oncology and Surgical Sciences, Padova; [2]Venetian Institute for Molecular Medicine, Padova; [3]Istituto di Ricerca di Biologia Molecolare (IRBM), Merck Sharp & Dohme Research Laboratories, Pomezia; [4]Aging Research Center (CeSI), G. d'Annunzio University Foundation, Chieti Scalo; [5]Department of Clinical and Experimental Medicine, Second University of Naples, Centro Regionale di Competenza in Genomica per la Ricerca Applicata, Napoli; [6]Department of Hematology, Oncology and Molecular Medicine, Istituto Superiore di Sanità, Rome; and [7]Istituto Oncologico Veneto (IOV), Padova, Italy

Telomerase reverse transcriptase (TERT) is a good candidate for cancer immunotherapy because it is overexpressed in 85% of all human tumors and implicated in maintenance of the transformed phenotype. TERT-based cancer vaccines have been shown to be safe, not inducing any immune-related pathology, but their impact on tumor progression is modest. Here we show that adoptive cell therapy with the use of high-avidity T lymphocytes reactive against telomerase can control the growth of different established tumors. Moreover, in transgenic adenocarcinoma mouse prostate mice, which develop prostate cancer, TERT-based adoptive cell therapy halted the progression to more aggressive and poorly differentiated tumors, significantly prolonging mouse survival. We also demonstrated that human tumors, including Burkitt lymphoma, and human cancer stem cells, are targeted in vivo by TERT-specific cytotoxic T lymphocytes. Effective therapy with T cells against telomerase, different from active vaccination, however, led to autoimmunity marked by a consistent, although transient, B-cell depletion in primary and secondary lymphoid organs, associated with alteration of the spleen cytoarchitecture. These results indicate B cells as an in vivo target of TERT-specific cytotoxic T lymphocytes during successful immunotherapy. (Blood. 2010;115:1374-1384)

Introduction

Attempts to treat experimental tumors with adoptive T lymphocyte transfer started in 1960, soon after the demonstration that the cellular arm of the immune system was responsible for tissue rejection.[1] The translation of this approach to the clinic, however, became possible when human tumor-infiltrating lymphocytes (TILs) could be expanded in vitro and injected back into cancer patients.[2] Only recently, however, an objective cancer regression was achieved in approximately 50% of patients with metastatic tumor after the introduction of host preconditioning by lymphodepletion before the treatment, followed by high-dose interleukin-2 (IL-2) to sustain in vivo expansion of T cells.[3,4] So far, this approach has been limited to melanoma patients, from whom TILs of known specificity are easily cultured in vitro, whereas for tumors other than melanoma the rescue of TILs is problematic.

Telomerase is considered an attractive target as universal antigen for the immunotherapy of cancer. Telomerase reverse transcriptase (TERT) is the protein component of the telomerase complex responsible for elongation of telomeres and plays an essential role in sustaining cancerous cell proliferation.[5] TERT is silent in most human somatic tissues but reactivated in 85% of tumors. Active immunization against telomerase and cancer vaccination clinical trials have been attempted that demonstrate little toxicity, but results concerning therapeutic efficacy are not conclusive.[6,7] Although T lymphocytes against telomerase were isolated and extensively characterized in vitro,[8,9] the use of adoptive cell therapy (ACT) with telomerase-specific lymphocytes has never been investigated. To evaluate therapeutic efficacy and determine the potential immunopathology associated with TERT-based ACT, we generated and analyzed the activity of TERT-specific CD8^{+} T cells.

Methods

Mice and cell lines

C57BL/6 mice were from Charles River Laboratories Inc. Transgenic adenocarcinoma mouse prostate (TRAMP) mice, a gift from N. M. Greenberg (Fred Hutchinson Cancer Research Center), were maintained in the mouse facility of Istituto Oncologico Veneto. Heterozygous TRAMP used in the experiments were obtained and screened as described.[10] C57BL/6-CD45.1[+] mice were a gift from M. P. Colombo (National Institutes of Tumors), *pmel*-1 TCR transgenic mice were a gift from N. Restifo (National Institutes of Health), and human leukocyte antigen (HLA)–A*0201-transgenic (HHD) mice were obtained by F. A. Lemonnier (Institut Pasteur) and maintained at Istituto di Ricerca di Biologia Molecolare. $Rag2^{-/-}\gamma_c^{-/-}$ were purchased form Taconic. Mice were treated in accordance with European guidelines (http://ec.europa.eu/environment/chemicals/lab_animals/legislation_en.htm). B16 melanoma cells were provided by N. Restifo (NIH). B16-B7.1 cells, genetically modified to express mouse B7.1 (provided by P. Della Bona, Istituto Scientifico San Raffaele) were cultured in the

The online version of this article contains a data supplement.

presence of G418 (0.5 mg/mL; Invitrogen). MBL-2 leukemia, MCA203 fibrosarcoma, MC38 colon carcinoma, EL-4 thymoma, and TC-1 lung carcinoma were all purchased from ATCC. TRAMP-C1 and TRAMP-C2 cell lines, established from prostate tumor of a TRAMP mouse, were provided by N. M. Greenberg (FHCRC). TRAMP-C1-B7.1 and TRAMP-C2-B7.1 transfectants were provided by S. Sartoris (University of Verona) and cultured with G418 (0.5 mg/mL) in Dulbecco modified Eagle medium high glucose (Invitrogen) in presence of 10^{-8}M dihydrotestosterone (Sigma-Aldrich), 5 µg/mL insulin (Sigma-Aldrich), 5% Nu serum IV (BD Biosciences), and 5% fetal bovine serum (Invitrogen). The 16.1 cytotoxic T lymphocytes (CTLs) recognizing the K^b-restricted epitope of β-galactosidase (β-gal$_{96-103}$: DAPIYTNV) were provided by M. P. Colombo (National Institutes of Tumors). The 293-A2 human embryonic kidney cell line, stably transfected to express the HLA-A2 class I molecule, was provided by J. C. Yang (National Institutes of Health). SW480 colon carcinoma, U266 myeloma, DG-75 Burkitt lymphoma, and TALL-1 acute T leukemia are all HLA-A2 positive whereas MOLT-3 acute T leukemia is HLA-A2 negative. All these cell lines were purchased from the ATCC. LNCaP is a human prostate carcinoma line deficient in HLA class I heavy-chain function provided by M. Colombatti (University of Verona).

Colon cancer stem cells characterization

Colon adenocarcinoma samples were obtained upon patients' informed consent and approval by the institutional research board of the University of Padua in accordance with the Declaration of Helsinki. Cell lines were obtained by mechanical and enzymatic dissociation of colon tumor samples and cultured as previously described.[11] Tumor spheres were mechanically dissociated, washed, and incubated with the specific antibody anti–HLA-A2 (BB7.2; BD Biosciences) or the isotopic control. Cells were then incubated with fluorescein isothiocyanate (FITC)–conjugated secondary antibody and analyzed by fluorescence-activated cell sorting (FACS; BD Biosciences). Expression of telomerase was determined by use of the TRAP assay (TRAPeze; Millipore). ^{33}P-radiolabeled polymerase chain reaction products were run on 10% nondenaturating polyacrylamide gel. The gel was dried and exposed to a sensitive Kodak film.

Plasmid and adenoviral vectors

The synthetic codon optimized sequence coding for TPA-human (h)TERT-LTB, which was cloned into vector pV1JnsA and used for immunization of HHD mice, was obtained by GENEART.[12] Two point mutations, D712A and V713I, were introduced to produce a catalytically inactive TERT enzyme.[13] The Ad6/mouse (m)TERT construct is deleted in the E1 and E3 viral regions. The sequence coding for mTERT is the native mTERT cDNA sequence obtained by Geron Corp. Mutations, D702V and V703I, into the murine TERT catalytic site, were introduced with the Stratagene quikchange multisite directed mutagenesis kit (Stratagene). mTERT cDNA was cloned SalI/SalI into pNEBAd6-CMVpA shuttle vector and sequenced. The plasmid pNEBAd6-CMVpA-mTERT was digested with PacI/PmeI and recombined to ClaI-linearized plasmid pMRK Ad6. The plasmid was cut with PacI to release the Ad ITRs and transfected in Perc-6 cells (Crucel). Ad6 vector amplification was carried out by serial passages and purified through CsCl gradient.

In vitro leukocyte cultures

Mouse TERT$_{198-205}$ CTLs were obtained from a mixed-leukocyte peptide culture set up with vaccinated TRAMP splenocytes (5×10^6) in presence of 0.1µM of mTERT$_{198-205}$ peptide (VGRNFTNL). Individual clones were obtained from the bulk population, after several cycles of restimulation, by limiting dilution. Human TERT CTLs were obtained from splenocytes (5×10^6) of vaccinated HHD mice grown in presence of 0.1µM of either hTERT$_{865-873}$ (RLVDDFLLV) or hTERT$_{30-38}$ (RLGPQGWRV) peptide. Human HER2/neu CTLs were obtained from HHD-vaccinated splenocytes stimulated with 1µM HER-2$_{369-377}$ (TYVPANASL) peptide. CTLs specific for both TERT and β-gal antigen were maintained by culture with γ-irradiated syngenic splenocytes pulsed with either 0.1µM TERT or 1µM β-gal$_{96-103}$ (DAPIYTNV) peptides. Gp100$_{25-33}$ CTLs derived from Pmel-1 splenocytes were stimulated once with 1µM specific hgp100$_{25-33}$ (KVPRNQDWL) peptide. Cultures were grown for 7 days in complete medium containing 20 IU/mL of recombinant human IL-2 (Novartis).

ACT

ACT in the metastatic model was performed after inoculation of C57BL/6 mice with 10^5 B16 tumor cells in the tail vein on day 0. On day 3, 5×10^6 of either mTERT-specific or β-gal–specific CTLs were administered intravenously. To sustain T-cell growth in vivo, recombinant human IL-2 (30 000 IU) was given twice a day intraperitoneally for 3 consecutive days. ACT in mouse-transplantable tumor models was performed in C57BL/6 mice after subcutaneous challenge with the following: 5×10^5 B16, 10^6 TRAMP-C2, 10^6 MCA203, 10^6 MC38, and 10^6 TC-1 cells. When the tumor area was approximately 10 mm^2, mice were sublethally irradiated (5 Gy). After 6 hours, 5×10^6 antigen-specific CTLs were injected intravenously. At the time of CTLs transfer, mice were injected intramuscularly with 5×10^8 PFU of the recombinant adenoviral vector coding for the relevant antigen recognized by transferred T cells and then treated with IL-2 as described previously. Tumors were measured on blind by the use of digital calipers. Mice were killed when the tumor area reached 100 mm^2.

TRAMP mice, 8 weeks of age, received ACT according the protocol described. The ACT was repeated when the mice were 13 and 18 weeks of age. In the last treatment, mice were not injected with recombinant adenovirus. Mice were killed when a macroscopic palpable tumor or signs of suffering were evident. In the human transplantable tumor models, Rag-2$^{-/-}$γ$_c^{-/-}$ mice were implanted subcutaneously with 10^6 SW480 colon cancer cells or with 10^6 DG-75 Burkitt lymphoma cells. When the tumor area was approximately 10 mm^2, mice were injected with 5×10^6 of hTERT-specific CTLs and IL-2, as described previously. In the human cancer stem cell model, Rag-2$^{-/-}$γ$_c^{-/-}$ mice were implanted subcutaneously with 5×10^5 tumor cells and at the same time injected intravenously with 5×10^6 of CTLs and IL-2, as described previously.

Analysis of the cell-mediated immune response

Released IFN-γ was measured by enzyme-linked immunosorbent assay (ELISA; Endogen Inc) after incubation of 10^5 CTLs for 24 hours with an equal amount of target cells.[14] ELIspot assay was performed by the use of peptide pools coding for hTERT. The immunogenic regions were experimentally identified by peptide deconvolution, as described.[14-16] Cytotoxicity was measured by ^{51}Cr release assay as described.[11] T- and B-cell blasts were obtained stimulating 25×10^6 splenocytes in complete medium containing either 5 µg/mL Concavallin A (ConA; Sigma-Aldrich) or 10 µg/mL lipopolysaccharide (LPS; Sigma-Aldrich) for 5 days. CD8$^+$ T cells in resting conditions were obtained by removing IL-2 from the culture medium.

Spectratyping analysis of TCR

The analysis was performed as described.[17] Analysis of TCR Vβ11 family representations in mTERT-specific bulk lymphocyte population was performed by the use of a TCR Vβ11-specific primer paired with a primer amplifying AJ41 region. This analysis allowed identification and sequencing of the CDR3 of the high-affinity clone. Primers specific for the CD3 region were then used for tracking the high-affinity TCR in the bulk population.

Cytofluorimetric evaluation of TILs

TILs were isolated by a mechanical separation followed by enzymatic digestion with 300 U/mL DNase, 0.1% hyaluronidase, and 1% collagenase buffer (Sigma-Aldrich). Cells were filtered through a 70-µm sieve and cultured with specific peptide in presence of IL-2 (20 IU/mL) for 18 hours. Intracellular staining (ICS) for interferon-γ (IFN-γ) was performed as described[11] by use of the following antibodies: anti–mouse CD8 PercP, anti–mouse Vβ8.1 FITC, anti–mouse Vβ11 FITC, or anti–mouse Vβ13 FITC anti–mouse IFN-γ PE monoclonal antibodies (mAbs). Cells were analyzed on FACSCalibur (BD Biosciences).

Characterization of murine bone marrow and spleen cells

Bone marrow (BM) cells obtained from femur and tibia were harvested from the diaphyses by flushing and from the epiphyses by bone crushing and mincing in RPMI 10% fetal bovine serum (Invitrogen) and then filtered through a 70-µm nylon strainer.[18] Spleens were prepared as described.[11]
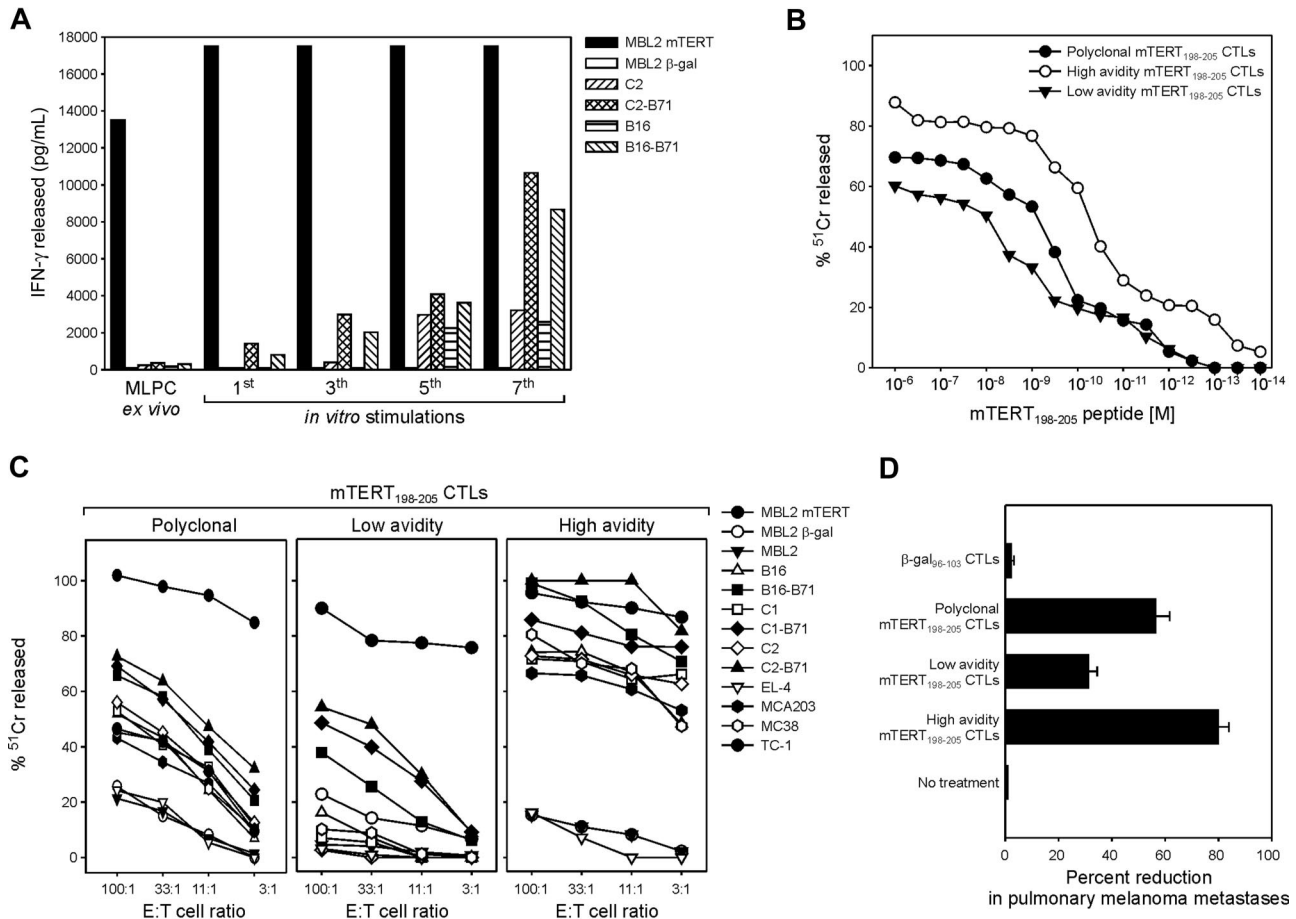
Figure 1. Functional characterization of mTERT$_{198-205}$-specific T lymphocytes. (A) Recognition of different syngenic tumor cells by mTERT-specific bulk T cells after repeated in vitro stimulations. T cells from different in vitro passages were incubated with an equal number of tumor cells for 24 hours and supernatants tested for released IFN-γ by ELISA. (B) Comparison of functional avidity of mTERT$_{198-205}$-specific bulk CTLs with high- and low-avidity CTL clones. The functional avidity was evaluated in ^{51}Cr release assay against MBL-2 target cells loaded with different mTERT$_{198-205}$ peptide concentrations at an effectors to target ratio of 10:1. (C) The mTERT-specific bulk T cells (left), the high-avidity (middle), and the low-avidity (right) clones were tested at different effectors to target cells ratios for cytotoxic activity against several different murine tumor cell lines by use of a ^{51}Cr release assay. The representative of 3 experiments is shown. (D) Therapeutic effectiveness of mTERT$_{198-205}$-specific CTLs. ACT was performed by the use of a melanoma metastatic model. Histograms show the mean ± SD of percentage reduction in the number of pulmonary metastases for melanoma-bearing mice inoculated with either mTERT-specific (polyclonal, high-avidity, and low-avidity) or β-gal–specific CTLs. Data are from 2 cumulative independent experiments. (Student t test: polyclonal mTERT vs β-gal, P = .001; low-affinity mTERT vs β-gal, P = .001; high-affinity mTERT vs β-gal, P < .001.)

A total of 5×10^6 cells/mL were stained with the following mAbs: anti–mouse immunoglobulin M (IgM; μ-chain specific)–FITC (Sigma-Aldrich), PE rat anti–mouse CD43 (BD), and allophycocyanin anti–mouse CD45R (B220; eBioscience) and analyzed by flow cytometry. Multistep gating was performed by use of the following gates: cytogram scatter gate to exclude debris and doublets (P1) and B220 gate on cells selected for B220$^+$ positivity (P2). This approach enabled us to identify multiple stages of B-cell development: pro-B cells (B220$^+$,CD43$^+$, IgM$^-$), pre-B cells (B220$^+$, CD43$^-$, IgM$^-$), and naive B cells (B220$^+$, CD43$^-$, IgM$^+$).[19]

Blood cell enumeration

Hematologic counts were performed (ADVIA 120). Cells were labeled with Anti-CD3 PerCP-Cy5, CD19 PE, DX5 FITC, and CD8 allophycocyanin-Cy7 after RBCs osmotic lyses for FACS analysis.[18] All antibodies were from BD Biosciences. Quantitative determination of mouse immunoglobulin was performed by the use of IgM and immunoglobulin G (IgG) ELISA kits (Alpha Diagnostic International Inc).

Histologic evaluation of tumors and tissues in TRAMP mice

The urogenital tract was removed at necroscopy and prepared for pathologic evaluation: tissues were fixed in paraformaldehyde/lysine/periodate at 4°C, infiltrated with 30% sucrose in phosphate-buffered saline overnight at 4°C, and frozen in OCT. Cryosections were stained with a standard

hematoxylin and eosin and then evaluated by 2 pathologists blinded to the treatment groups.[20,21] The presence of normal tissue, low-grade prostate intraepithelial neoplasia (LG-PIN), high-grade PIN (HG-PIN), and adeno-carcinoma was scored. The occurrence of poorly differentiated carcinomas (PDCs) also was evaluated.

Several organs (liver, lungs, small and large bowel, kidneys, heart, testis, brain, and spleen) were collected at the time of mouse death to assess for possible treatment toxicity. Tissues were fixed in 10% buffered formalin and embedded in paraffin. Histopathologic evaluation was performed on standard hematoxylin-and-eosin sections.

Immunohistochemistry analysis of spleen B cells

Longitudinal sections of the spleen, close to the hilar region, were examined to increase the amount of lymphoid tissue available for the assessment of B cells. Cryosections were fixed in cold acetone washed in Tris-buffered saline and incubated with a Background Sniper (Biocare Medical) before the incubation with the rat anti–mouse CD45R Ab (BD Biosciences), followed by the secondary Ab goat anti–rat IgG (Jackson ImmunoResearch Laboratories). The staining was developed by incubation with Neutravidin alkaline phosphatase-conjugated (Thermo Scientific) followed by the Vulcan Fast Red (Biocare Medical) chromagen. Sections were finally counterstained in hematoxylin, mounted in Eukitt (Bioptica) and examined
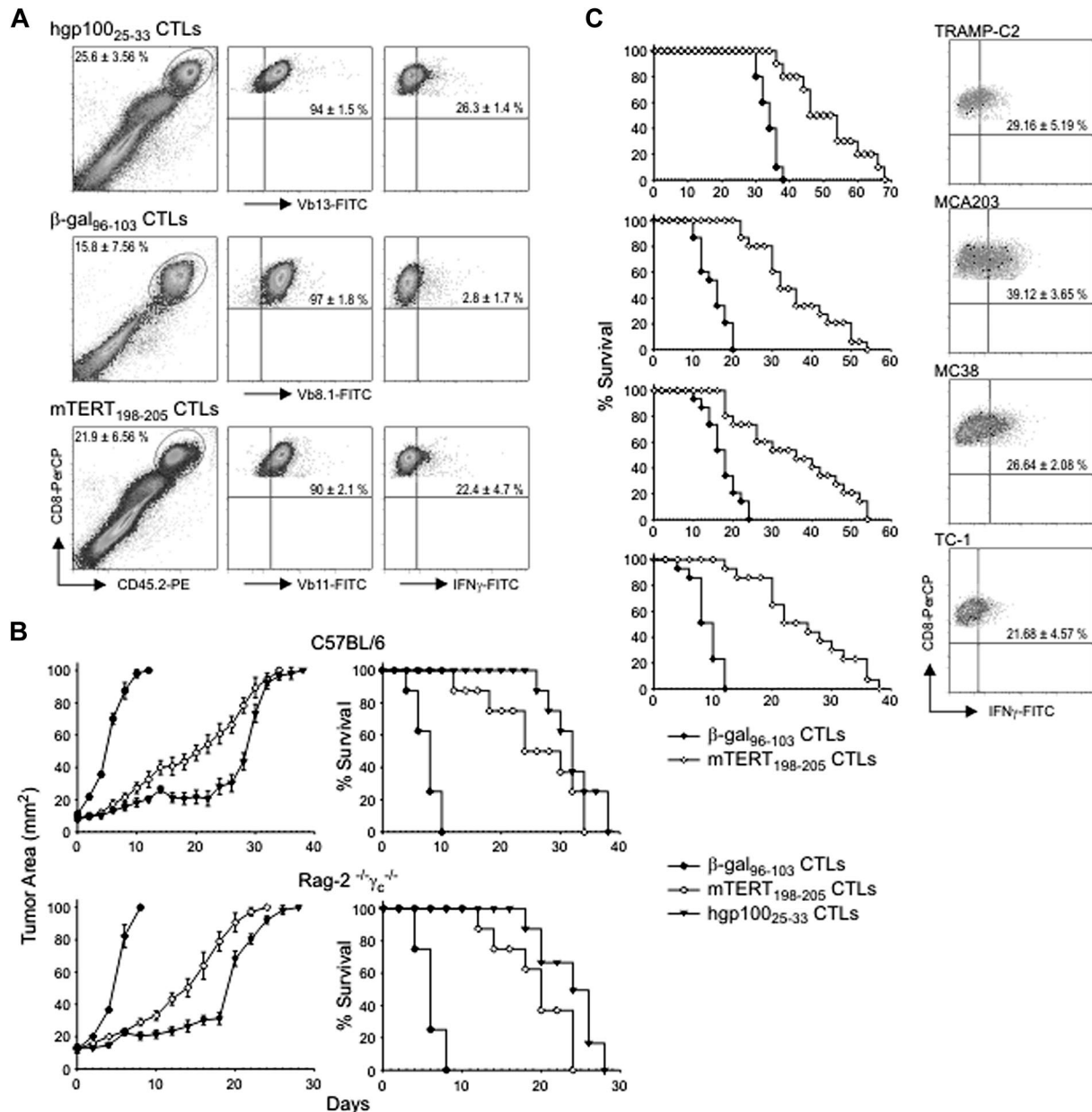
Figure 2. ACT with mTERT$_{198-205}$ CTLs is effective in several transplantable tumor models. (A) Evaluation of CTL ability to traffic to tumors. B16 melanoma cells were injected in C57BL/6-CD45.1$^+$ mice. When the tumor area was ~ 10 mm^2, mice received hgp-100$_{25-33}$-, mTERT$_{198-205}$-, or β-gal$_{96-103}$–specific CTLs. At 4 days after transfer, tumors were harvested for TIL analysis. Transferred CTLs were tracked as CD8$^+$/CD45.2$^+$ cells (left). CD8$^+$/CD45.2$^+$ cells were then evaluated for the staining with specific mAbs for TCR Vβ chain: anti-Vβ8.1 for β-gal$_{96-103}$, anti-Vβ11 for mTERT$_{198-205}$, and anti-Vβ13 for hgp-100$_{25-33}$ CTLs (middle). The activation status of TILs was evaluated by ICS for IFN-γ after ex vivo stimulation (right). Data are mean ± SD of 3 independent experiments. (B) Therapeutic effectiveness of ACT with the use of mTERT$_{198-205}$-specific CTLs in a melanoma model. C57BL/6 mice (top) and Rag-2$^{-/-}$γ$_c$$^{-/-}$ mice (bottom) were implanted with B16 cells. Survival and tumor area are plotted from 3 cumulative experiments (n = 15). Mantel–Haenszel statistic analysis for survival: for C57BL/6 model, hgp-100 vs β-gal, P = .001; mTERT vs β-gal, P = .001; mTERT vs hgp-100, P = .16; for Rag-2$^{-/-}$γ$_c$$^{-/-}$ mice, hgp-100 vs β-gal, P = .001; mTERT vs β-gal, P = .001; mTERT vs hgp-100, P = .29. (C) Therapeutic effectiveness of ACT by use of mTERT$_{198-205}$-specific CTLs in 4 tumor models. C57BL/6 mice were implanted with TRAMP-C2, MCA203, MC38, or TC-1 cells and treated as described in the melanoma model. TILs were evaluated by ICS for IFN-γ after ex vivo stimulation (right). Survival from 3 cumulative experiments (n = 15) is shown (left). Mantel-Haenszel statistics for mTERT vs β-gal comparison: C2-TRAMP, P = .027; MCA203, P = .001; MC38, P = .016; TC-1, P = .001. Transferred TILs were tracked, and IFN-γ and CD8 staining is shown on cells gated for CD45.2$^+$ T cells (right). Data are mean ± SD of 3 independent experiments.

by 2 pathologists blinded to the treatment groups. The number of B cells was evaluated by giving a score of positivity from 1 to 5 per field.

Statistical analysis

The Wilcoxon Mann-Whitney U test was used to examine the null hypothesis of rank identity between 2 sets of nonparametric data. The Student t test was used to compare parametric groups. Kaplan-Meier plots and the Mantel-Haenszel test were used to compare survival of mice. The Fisher exact test was used to compare frequencies and analysis of variance test for pairwise comparisons. P values are all 2-sided.

Results

In vitro culture enriches high-avidity T lymphocytes specific for mTERT recognizing several syngenic tumor cells

C57BL/6 mice were vaccinated with mTERT DNA plasmid, and T cells specific for K^b-restricted, TERT epitope (mTERT$_{198-205}$) were enriched from splenocytes by stimulation with the peptide.[14] Specific recognition was determined by IFN-γ release.

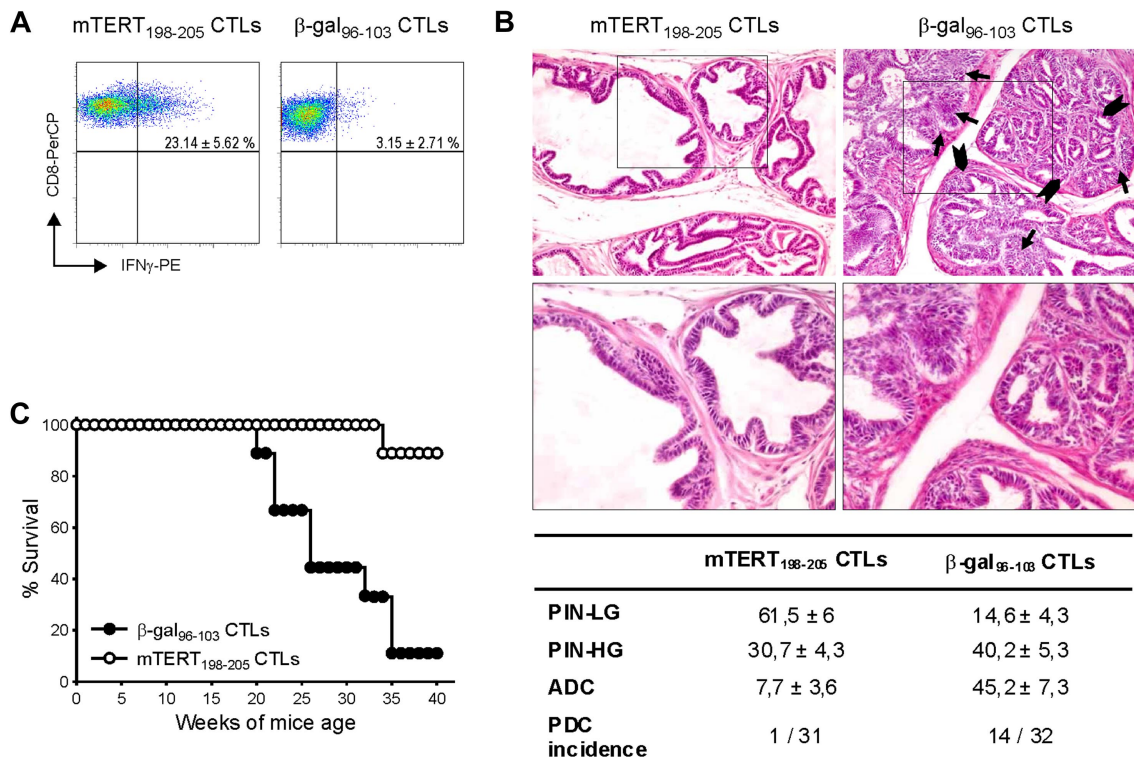|	mTERT$_{198-205}$ CTLs	β-gal$_{96-103}$ CTLs
PIN-LG	61,5 ± 6	14,6 ± 4,3
PIN-HG	30,7 ± 4,3	40,2 ± 5,3
ADC	7,7 ± 3,6	45,2 ± 7,3
PDC incidence	1 / 31	14 / 32

Figure 3. Therapeutic impact of mTERT-based ACT on TRAMP mice. (A) Activated CTLs are able to traffic to prostate tumor. TRAMP mice were subjected to 3 consecutive ACTs and, 4 days after last ACT, prostate tumors were harvested and stained to track either mTERT-specific (CD8$^+$/Vβ11$^+$) or β-gal–specific(CD8$^+$/Vβ8.1$^+$) CTLs. IFN-γ and CD8 staining is shown on cells gated for specific Vβ expression. Data are mean ± SD of 3 mice. (B) Representative histologic pictures of prostates of TRAMP mice treated with either mTERT$_{198-205}$–specific (left) or control CTLs (right) at 24 weeks of age. Prostate in majority of mTERT-specific CTL treated mice is occupied by PIN-LG foci, showing normal sized glands lined by few and flat layers of atypical cells. In control mice, PIN-HG–affected prostatic ductules appear enlarged and distorted by crowded intraluminal papillae coalescing into cribriform structures (arrowheads). Numerous solid nests of adenocarcinoma (arrows) focally invade base membrane (see also insert; magnification: top panels, ×200; bottom panels, ×400). The table summarizes the prostate areas occupied by different tumor lesions. Values are expressed as mean ± SE. The incidence of PDC also is indicated. Wilcoxon rank sum test: PIN-LG is more represented in TERT-specific CTL-treated animals (P = .001); PIN-HG is not statistically different; adenocarcinoma (ADC) is more represented in β-gal–specific CTL-treated mice (P = .001). The incidence of PDC was evaluated with the Fisher exact test (P = .001). (C) Overall survival of TRAMP mice undergoing ACT. Survival curves from TRAMP mice treated with either mTERT-specific (n = 9) or β-gal–specific (n = 10) CTLs are shown. Kaplan-Meier analysis: mTERT vs β-gal, P < .001.

Recognition of target MBL-2 cells, loaded with the mTERT$_{198-205}$ peptide, was detectable already ex vivo with the use of effectors splenocytes isolated from immunized mice; however, recognition of TERT peptide naturally processed by syngenic tumor cells, like TRAMP-C2 and B16, was acquired only after several cycles of in vitro stimulation (Figure 1A). Two T-cell clones derived from the bulk population were then isolated and characterized. To have an accurate comparison of the overall T-cell avidity, the 2 clones and the bulk T-cell population were tested for the killing activity on MBL-2 cells loaded with titrated amounts of TERT$_{198-205}$ peptide (Figure 1B). The CTL killing curve placed the polyclonal bulk population exactly between the 2 clones. Specific recognition of tumor cells determined by lytic activity was then investigated (Figure 1C). The high-avidity clone and the bulk population, although to a lower extent, killed several epithelial (B16, TRAMP-C2, TRAMP-C1, MC-38, and TC-1) and the mesenchymal (MC-203) tumors, whereas cells derived from T-cell leukemias, like MBL2 and EL-4, were not recognized (Figure 1C). The low-avidity CTL could only recognize target cells engineered to express the costimulatory molecule B7.1 on cell surface, as previously shown for other low-avidity CTLs.[14,17] Comparable results were obtained by the use of IFN-γ release assay to assess the recognition patterns (data not shown). These results were also confirmed in vivo in a metastatic B16 melanoma model (Figure 1D). Pulmonary metastases were established by the intravenous injection of B16 cells and, after 3 days, T cells were transferred without any host preconditioning. The high-avidity clone brought a reduction of more than 80% in the number of metastases formed, the low-avidity clone reduced metastases by only 30%, and the bulk population resulted in approximately 60% reduction.

The high-avidity anti-TERT clone was the natural candidate for ACT experiments. However, all the mTERT-specific clones we isolated experienced a growth crisis and could not be further expanded. The bulk population instead could be maintained in culture with the pattern and the strength of tumor recognition basically unchanged for 24 months (supplemental Figure 1A, available on the *Blood* website; see the Supplemental Materials link at the top of the article). Molecular analysis by spectratyping of the TCRs in the bulk T-cell population, after each stimulation cycle, revealed a progressive accumulation of TCR Vβ11, sharing the same CDR3 length of the high avidity clone (supplemental Figure 1B). Moreover, by quantitative polymerase chain reaction, by using clonotypic primers designed on the basis of the high-avidity clone (CDR3 sequence accession number EF52405),[17] we observed a progressive expansion of this specific clonotype that accounted for 70% of the total TCR Vβ11 present in the T-cell polyclonal line (supplemental Figure 1C). This pattern was stable for 24 months of continuous in vitro passages, indicating that the polyclonal CTLs were functionally and molecularly stable.

Figure 4. Immunopathology related to TERT-based ACT: reduction of blood cells. (A) WBC counts in TRAMP mice treated with ACT. Blood was collected from mice euthanized at the 24th week. Average values and SD are shown for total WBCs, granulocytes, lymphocytes, and monocytes (mTERT n = 27; β-gal n = 22). Wilcoxon rank sum test mTERT vs β-gal: WBC, $P < .001$; lymphocytes, $P < .001$; granulocytes, $P = .09$; monocytes, $P = .01$. (B) Average values and SD for lymphocytes subpopulations analyzed by FACS are shown (mTERT n = 10; β-gal n = 8). Wilcoxon rank sum test mTERT vs β-gal: CD3$^+$, $P = .001$; CD3$^-$CD19$^+$, $P = .001$; CD3$^+$CD8$^+$, $P = .001$; CD3$^-$DX5$^+$, $P = .005$. (C) IgG and IgM serum levels in the 2 treated groups are shown. (D) mTERT$_{198-205}$-specific CTLs recognize normal B cells. CTLs were incubated with autologous LPS-induced blast cells, ConA-induced blast cells, or with CD8$^+$ T cells under activating or resting conditions. Data are mean ± SD of 2 independent experiments. Statistically significant differences (analysis of variance, $P < .001$) between B-cell and T-cell recognition was found at the effector/target cell ratio of 200:1.
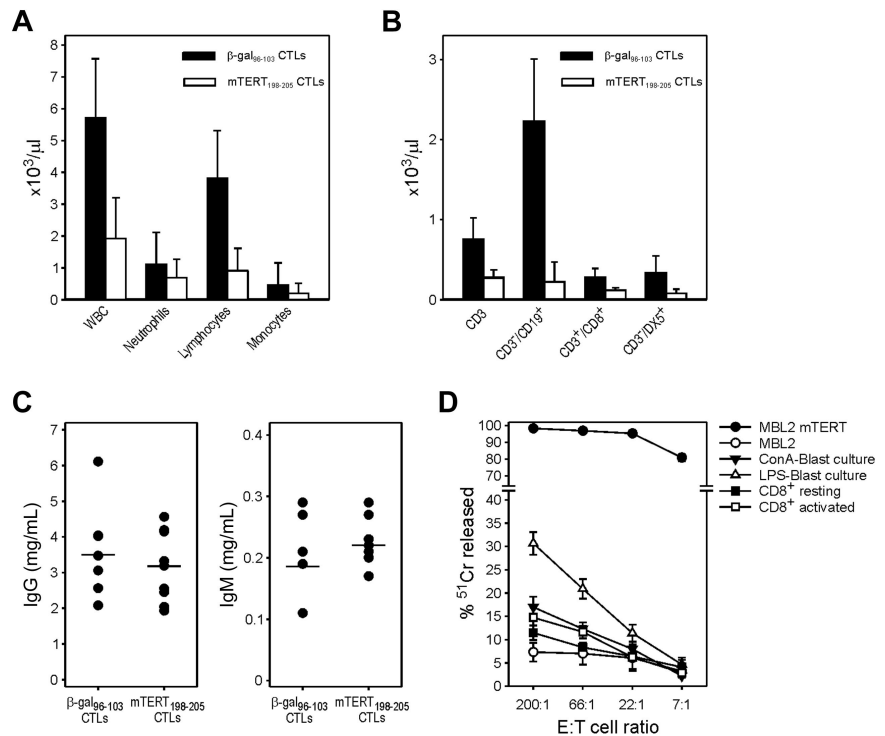
ACT with mTERT-specific CTLs controls tumor growth in several transplantable models

Melanoma has been extensively used to validate ACT.[22] We compared the in vivo activity of mTERT-specific CTLs with an example of successful ACT toward tumor-associated antigens, the CTLs recognizing hgp-100 melanoma antigen (hgp-100$_{25-33}$) derived from Pmel-1 TCR transgenic mice,[23] whereas CTLs specific for β-gal were used as a negative control. Melanoma-bearing mice were lymphodepleted by nonmyeloablative irradiation, immunized on the same day of ACT with a recombinant adenoviral vector coding for the specific antigen, and given IL-2 afterward, as previously established.[23] After 4 days, TILs were isolated from the melanoma mass and distinguished from recipient lymphocytes by the expression of CD45.2 congeneic marker. From 15% to 25% of CD8$^+$-infiltrating T lymphocytes were CD45.2$^+$ (Figure 2A). The TCR Vβ chains of the various CTLs were known, and it was therefore possible to track specifically transferred T cells in the tumor mass. More than 90% of CD8$^+$/CD45.2$^+$ T cells expressed the expected TCR Vβ chain, representative of the transferred population (Figure 2A). Moreover, ICS for IFN-γ showed that T lymphocytes specific for the tumor antigens gp100 and TERT were responsive to antigen stimulation, whereas β-gal–specific lymphocytes were unresponsive (Figure 2A).

An equal delay in tumor growth and increased mouse survival was achieved with the transfer of both gp100- and TERT-specific CTLs (Figure 2B). The same therapeutic activity was observed in Rag-2$^{-/-}$γc$^{-/-}$ mice, which are genetically lymphodepleted and therefore do not require any conditioning regimen before ACT (Figure 2B).[24] In summary, the therapeutic effect of TERT-based ACT with polyclonal CTLs on melanoma-bearing mice was basically indistinguishable from that of T cells possessing a clonotypic TCR specific for a well-characterized melanoma antigen.

To address the relevance of anti-TERT ACT for tumors other than melanoma, 4 additional transplantable models were evaluated. TILs were analyzed by ICS for IFN-γ by tracking transferred lymphocytes by their TCR Vβ11 chain expression. T cells present in the tumor mass showed a percentage of T lymphocytes responsive to mTERT ranging from approximately 20% (TC-1) to 40% (MCA-203). In all these models, significant prolongation of survival was observed (Figure 2C).

Adoptive transfer of mTERT-specific CTLs controls tumor progression in TRAMP mice

Tumors arising in genetically engineered mice are considered suitable models for evaluating results transferable to a clinical setting. The TRAMP mouse model is engineered to express SV40 large T antigens, preferentially in the prostate epithelium to develop prostate tumors.[10] We previously demonstrated that mTERT is overexpressed in transformed prostates.[14] Because the TRAMP model is characterized by the continuous formation of new cancerous lesions, ACT was repeated 3 times at 8, 13, and 18 weeks of age. Nonmyeloablative irradiation regimen was performed before each ACT. After the first 2 adoptive CTL transfer, mice were also immunized with the antigen-encoding adenovirus and IL-2 was injected after all ACT. Transferred CTLs were monitored within the tumor, 4 days after the last ATC. Activated T cells producing IFN-γ were found only in prostates of mice inoculated with TERT-specific CTLs (Figure 3A). Pathologic evaluation and image analysis of prostates, examined at 24 weeks of age, is shown in Figure 3B. A total of 7.7% of prostate area is occupied by adenocarcinoma in the group treated with mTERT-specific CTLs, compared with 45.2% in those receiving the β-gal–specific CTLs. Moreover, only in 1 of 31 animals analyzed, a poorly differentiated carcinoma was observed, whereas 14 of 32 had PDC in the control group. On the contrary, LG-PIN areas, which represent early lesions, were more numerous in prostatic tissue of mice treated with mTERT-specific CTLs than in control group. It seems that in this model ACT resulted in accumulation of very early lesions by blocking their progression to more advanced tumors. A second group of TRAMP mice was monitored till appearance of palpable
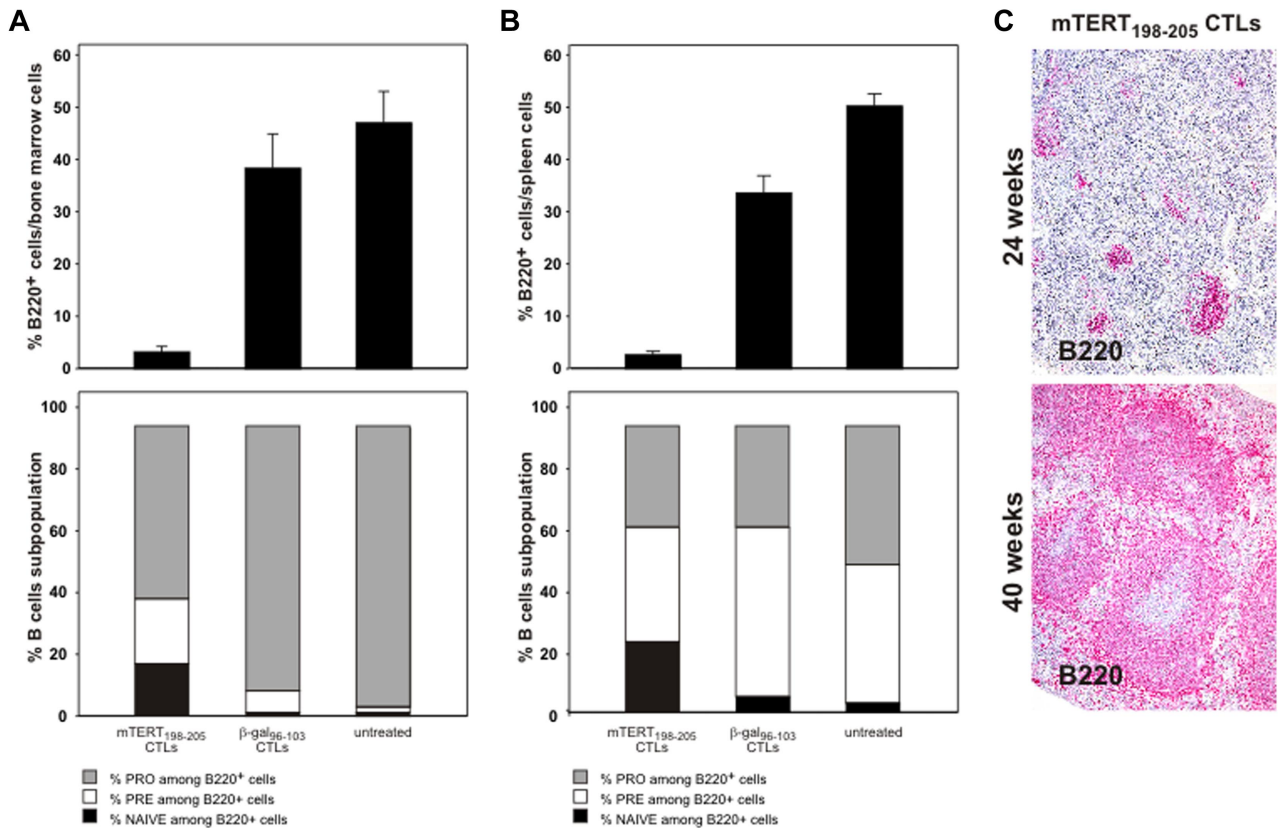
Figure 5. B-cell reduction induced by TERT CTLs is transient. (A) BM B-cell subsets after ACT treatment. C57BL/6 mice (n = 6/group) received ACT, and BM was collected 5 days later. B220 staining identifies BM B cells (top). Wilcoxon rank sum test: β-gal vs mTERT, P = .005. B-cell subpopulations were then characterized (bottom) as follows: pro-B: $B220^+/CD43^+/IgM^-$; pre-B: $B220^+/CD43^-/IgM^-$; naive $B220^+/CD43^-/IgM^+$. Wilcoxon rank sum test: pro-B mTERT vs pro-B β-gal, P = .005. (B) Spleen B-cell subsets after ACT treatment. C57BL/6 mice (n = 6/group) received ACT and spleens were collected 5 days later. B220 staining shows a profound B-cell depletion in mice treated with TERT ACT. Wilcoxon rank sum test: β-gal vs mTERT, P = .002. Staining for expression of CD43 and surface IgM allowed characterization of B-cell subpopulations (pro-B: $B220^+/CD43^*/IgM^-$; pre-B: $B220^+/CD43^-/IgM^-$; naive: $B220^+/CD43^-/IgM^+$). Wilcoxon rank sum test: pro-B mTERT vs pro-B β-gal, P = .005. (C) B220 staining of TRAMP mice spleens by IHC. Spleens were collected at 24 weeks (mTERT n = 18 and β-gal-n = 16) or at 40 weeks of age (mTERT n = 6). Samples were scored for the B220 positivity with a scale from 1 to 5. Wilcoxon rank sum test: mTERT at 24 weeks vs β-gal at 24 weeks, P = .007; mTERT at 40 weeks vs β-gal at 24 weeks, P = .8; mTERT at 40 weeks vs mTERT at 24 weeks, P = .05.

macroscopic tumor. A clear impact of mTERT-based ACT on overall survival was observed (Figure 3C).

TERT-based ACT induces B-cell depletion

Mice treated by repeated ACT with mTERT-specific CTLs did not show any clear symptom related to possible immune adverse events. At 24 weeks of age, after 3 cycles of ACT, mice were examined to enumerate blood cells and evaluate histomorphologic changes in different organs. Red cell counts and hemoglobin were within the normal range in both groups (data not shown). White blood cell (WBC) counts were instead reduced in most of the mice treated with mTERT-specific CTLs but not in mice receiving control CTLs. The WBC reduction was mainly caused by decreased numbers of circulating lymphocytes (Figure 4A). The absolute number of circulating T ($CD3^+$), B ($CD3^-CD19^+$), and natural killer ($CD3^-DX5^+$) cells were affected by TERT-based ACT and significantly reduced compared with controls (Figure 4B). However, the effect was more pronounced for B lymphocytes; in fact, the relative numbers of T lymphocytes was even increased compared with controls because of the prominent B-cell depletion (supplemental Figure 2). The reduction in B cells did not compromise the concentration of serum IgM and IgG antibodies (Figure 4C). A susceptibility of B cells to in vitro killing by CTL specific for human (h)TERT was previously described.[25] We thus tested the ability of mTERT-specific CTLs to recognize and kill either

LPS-induced (B-cell) or ConA-induced (T-cell) blasts. To achieve lytic activity against normal activated B cells, a very high CTL-to-target-cell ratio was required (200:1), but nevertheless specific lysis of B-cell blast was observed whereas T cells were marginally recognized (Figure 4D).

B-cell reduction induced by TERT CTLs is transient

To determine the long-term impact of ACT, the in vivo recovery potential of B cells was evaluated. BM was obtained 5 days after ACT. An important reduction of whole B cells identified by B220 marker was demonstrated in mice treated with mTERT-specific CTLs (Figure 5A), whereas mice transferred with β-gal–specific CTLs showed instead a prompt B-cell recovery, reaching 5-day postirradiation frequencies similar to untreated mice. To monitor the regenerative B-cell activity, markers for B-cell subpopulations were further analyzed.[19] A relative increase in very early B cells precursors (pro-B) was observed 5 days after mTERT-based ACT compared with either β-gal–based ACT or untreated mice, which is indicative of compensative-cell repopulation (Figure 5A). A similar picture emerged from the analysis of the spleens in the same mice (Figure 5B). Indeed, spleens obtained from 24-week-old TRAMP mice receiving mTERT-based ACT showed a reduction of $B220^+$ B cells and an altered architecture compared with control mice (Figure 6). However, a complete recovery of the spleen $B220^+$-cell population and cytoarchitecture normalization were found in mice
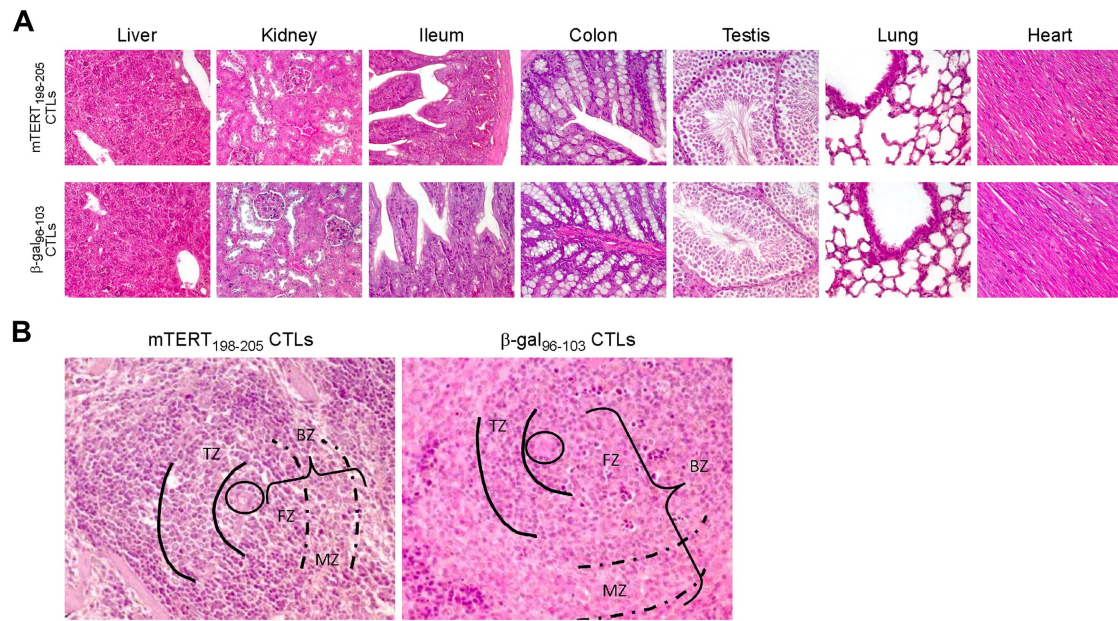
Figure 6. Immunopathology related to TERT-based ACT: tissue histology. (A) Both mTERT-specific (top) and β-gal–specific (bottom) CTL-treated mice did not show any morphologic alteration of liver, kidney, small and large intestine, testis, lungs, and heart as assessed by histologic analysis. Liver sections from treated and control mice showed typical polygonal arrangement of lobules. Portal triads were regularly distributed; neither portal nor centrolobular degeneration was present. Renal specimens of both experimental groups showed normal renal cortex. There were no evidence of glomerular hypercellularity or an increase in thickness of capillary walls, nor was there flogosis or fibrosis of tubulointerstitial compartment. Small (ileum) and large (colon) intestine sections appeared normal: there was no damage of the villous architecture or glandular distortion, and there were no flogistic or fibrotic alterations of the lamina propria. In the testis of mTERT-specific CTL-treated and control-treated mice, seminiferous tubules were normal in size and number; there were no alterations of spermatogenic cell maturation. Healthy lung parenchyma from mTERT-specific CTL-treated and control groups was composed by flat walled alveoli with interposed thin layer of connective tissue and normal bronchial tree. No pathologic alterations were found in heart: normal myocardium composed of striated muscle fibers is shown. (B) Spleen of mTERT-specific CTL-treated mice showed impaired architecture respect to control samples: B-cell rich outer compartment of periarteriolar lymphoid sheets (parentheses, BZ) had a reduced thickness of both follicular (FZ) and marginal zones (dashed lines, MZ). T-cell inner zone (solid lines, TZ) was normal in both groups.

euthanized at 40 weeks of age (Figures 5C and 6A). With the exception of the spleen, histomorphologic analysis of other tissues did not show any remarkable alteration, even in tissues with high cell turnover like the intestine and testis (Figure 6).

T lymphocytes specific for hTERT$_{865-873}$ control in vivo HLA-A2$^+$ tumor growth and abolish neoplastic development from human cancer stem cells
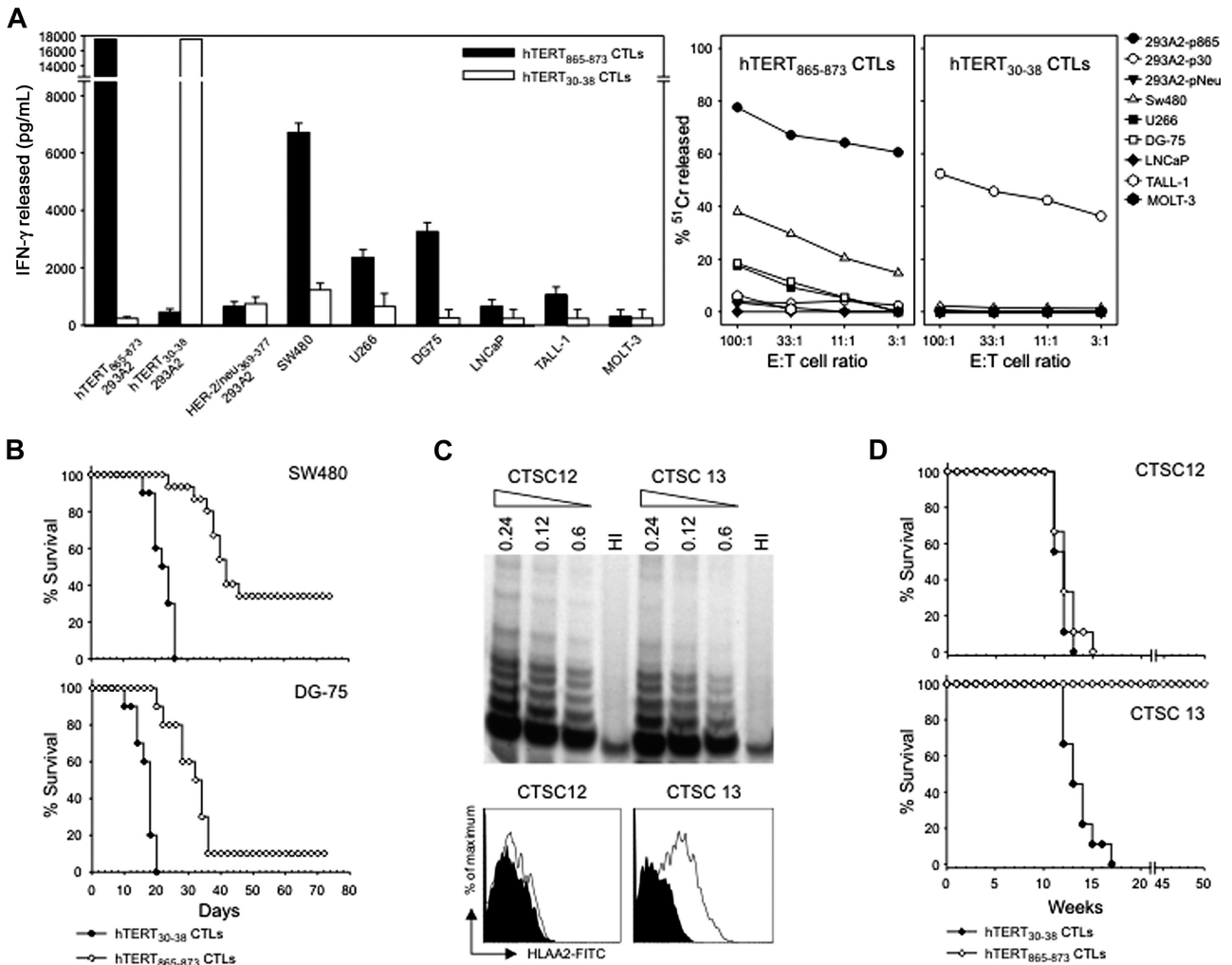
HLA-A2 transgenic mice were immunized with a plasmid encoding hTERT, and immunogenic HLA-A2–restricted epitopes were experimentally identified as described.[26] The 3 hTERT immunogenic regions that were found corresponded to epitopes already described (supplemental Figure 3A-C).[25,27,28] T cells specific for the 2 epitopes hTERT$_{865-872}$ and hTERT$_{30-38}$, showing the strongest reactivity ex vivo (supplemental Figure 3D), were further enriched from splenocytes through repeated peptide stimulations. Specific recognition of 293 cells stably transfected with HLA-A2 molecule (293-A2) and loaded with the relevant peptides was readily demonstrated ex vivo (supplemental Figure 3C). However, repeated stimulation cycles were necessary for the selection of a polyclonal T-cell population able to produce IFN-γ when incubated with a panel of human tumor cells lines. Whereas T cells reactive against hTERT$_{865-872}$ epitope acquired this capacity, T cells recognizing hTERT$_{30-38}$ never did (Figure 7A). Only prostate-derived cells LnCap, deficient in the class I HLA heavy chain, were never recognized. In agreement with mouse results, T cells specific for hTERT$_{865-872}$ did not recognize acute T-cell leukemic lines TALL-1 and MOLT-3, HLA-A2$^+$ and HLA-A2$^-$, respectively. ACT with hTERT-specific T cells was then performed in Rag-2$^{-/-}$γ$_c^{-/-}$ mice engrafted with human HLA-A2$^+$ tumors (either SW480 colon

carcinoma or Burkitt lymphoma cell-line DG 75). Figure 7B shows survival curves of mice injected subcutaneously with either SW480 or DG-75 tumor cells and passively transferred with hTERT-specific CTLs. Prolonged survival and complete cure in some mice were observed.

We finally asked whether hTERT recognition might also affect the pool of cancer stem cells. Cancer stem cells were thus isolated from colon adenocarcinoma surgical specimens.[11] Cells were characterized for hTERT expression by TRAP assay and for HLA-A2 presence by FACS analysis. Two cancer stem cell preparations having comparable levels of telomerase activity were selected on the basis of HLA-A2 positivity (Figure 7C). CTLs were transferred on the same day of cancer stem cell inoculation to verify the efficacy of active immunotherapy directly on cancer stem cell tumorigenicity. HLA-A2 tumor stem cells did not grow in any of the mice treated with the hTERT$_{865-873}$-specific CTLs, whereas the hTERT$_{30-38}$-specific CTLs were unable to control tumor development (Figure 7D). The selectivity of the immune attack was further demonstrated by the observation that in vivo growth of the HLA-A2–negative cancer stem cells could not be prevented by hTERT$_{865-873}$-specific CTLs (Figure 7D).

Discussion

ACT represents, at the moment, the most promising immunotherapy approach for cancer treatment.[29] Telomerase is a tumor-associated antigen with features making it particularly attractive for ACT: it is shared among several tumor types, plays a key role in sustaining cancer progression, and is associated with a poor

Figure 7. Functional characterization of HLA-A2–restricted CTLs specific for hTERT. (A) hTERT CTLs were analyzed after 10 cycles of stimulation with either hTERT$_{865-873}$ or hTERT$_{30-38}$ peptides. Recognition of HLA-A2 tumor cells by hTERT-specific T cells. Polyclonal CTLs specific for hTERT$_{865-873}$ and hTERT$_{30-38}$ epitopes were tested both in IFN-γ ELISA (left) and in ^{51}Cr release assay (right). 293-A2 cells were pulsed with the hTERT peptides as positive control or with HER-2/neu$_{369-377}$ peptide as a negative control. Data are mean ± SD of 3 independent experiments. (B) Therapeutic effectiveness of ACT by use of hTERT$_{865-873}$-specific CTLs. Rag-2$^{-/-}$γc$^{-/-}$ mice were implanted with either SW480 or DG-75 tumor cells and when tumor area was ∼10 mm^2, either hTERT$_{865-873}$-specific or hTERT$_{30-38}$-specificCTLs were injected. Data are the summary of 3 cumulative experiments (n = 15/group). Mantel–Haenszel statistics: hTERT$_{865-873}$ vs hTERT$_{30-38}$, $P <$ .001. (C) Characterization of cancer stem cells isolated from colon adenocarcinoma surgical specimens. Telomerase activity was measured by TRAP assay (left). Dilutions of TRAP products were loaded on 10% polyacrylamide gel. HI indicates heat-inactivated samples. Expression of HLA-A2 was analyzed by FACS after staining with anti-human HLA-A2 mAb or isotype control (right). (D) Cancer stem cells are in vivo target of hTERT$_{865-873}$-specific CTLs. Survival curves of Rag-2$^{-/-}$γc$^{-/-}$ mice implanted with CTSC12 (HLA-A2$^-$) or CTSC13 (HLA-A2$^+$) cells. Mice were then injected with either hTERT$_{865-873}$-specific or hTERT$_{30-38}$-specific CTLs. Data are from 3 cumulative experiments (n = 5/group). Mantel–Haenszel statistics: CTSC 12: hTERT$_{865-873}$ vs hTERT$_{30-38}$, $P =$ .43; CTSC 13: hTERT$_{865-873}$ vs hTERT$_{30-38}$, $P <$ .001.

prognosis.[30,31] During the past years, several authors[8,32] have shown that TERT is immunogenic both in vivo and in vitro, and clinical trials[6,7] based on hTERT vaccination have been started in patients with advanced cancer. Experimental data have conclusively shown that cancer vaccination is safe but the overall impact on established tumors needs to be improved. We recently described that DNA-based vaccination in TRAMP mice prevented the progression to adenocarcinoma but had no effect on the incidence of PDC and a modest influence on the overall survival.[14] On the contrary, we describe here, for the first time, that ACT with anti-TERT CTLs has a dramatic effect on both PDC appearance and mouse survival (Figure 4). This finding is relevant for human pathology. It is more and more evident, in fact, that PDC in TRAMP mice resembles the human androgen-independent prostate cancer,[10,33] which cannot be considered a simple progression from the adenocarcinoma but it might represent a distinct nosologic

identity. Androgen-independent tumors do not respond to treatments, and prognosis has not truly changed in the last 50 years.[34]

As anticipated from mouse studies on melanoma antigens,[35] it was expected that therapeutic benefits by TERT-based ACT could be associated with immunopathology and autoimmunity. Mice treated with repeated ACT of TERT CTLs did not show any clear symptom related to possible immune adverse events. At 24 weeks of age mice did not show relevant changes of tissues architecture, even in the case of tissues with a high proliferative capacity like the intestine, the only exception being the spleens where an altered cytoarchitecture was noticed in most of treated mice. These findings related to the reduced WBC counts with predominant B-cell depletion, also confirmed by spleen immunostaining for B220-positive cells. It was surprising that side effects were limited to B cells, given the widespread expression of mTERT in mice. B-cell progenitors are indeed very sensitive to low doses of the

preparative irradiation and undergo very rapid regeneration shortly thereafter to repopulate BM.[36] B-cell homeostatic proliferation, different from T cells, is independent from antigen binding and driven by environmental factors.[37,38] At the time of ACT, B cells are in an explosive regeneration phase, likely with very high levels of telomerase turnover and thus become a favorite target of the immune attack. Moreover, a greater susceptibility of activated mouse and human B cells, compared with activated T cells, to telomerase-specific CTLs was shown here in vitro. All these observations suggest that the major factor determining expression of TERT peptides on cell surface and susceptibility to the immune attack is likely not the steady-state level of telomerase expression but telomerase turnover, ultimately linked with the proliferative activity. Thus differences in TERT expression between human and mice may be not so crucial, and a similar outcome is likely to occur in humans as in mouse experimental models. Moreover, if anything, the wider expression of telomerase in mouse tissues would pose greater concerns about immune tolerance than in humans.

In agreement with a prolonged activity of adoptively transferred CTLs, TERT-specific but not β-gal–specific CTLs could be detected 6 weeks after last ACT (supplemental Figure 4). However, complete B-cell repopulation of the spleens was demonstrated, in a group of ACT-treated mice, 22 weeks after the last TERT-based ACT (Figure 5). On the whole, these data suggest a long-lasting immune destruction of intermediate B cells with high proliferative rate but also a complete recovery of the B-cell compartment after a few months. However, B-cell counts in the blood might actually provide a surrogate marker to monitor the effectiveness and duration of TERT-based ACT in cancer patients. Despite the lack of mature B cells, however, both IgM and IgG remained within the normal range in mice receiving TERT-based ACT. Moreover, B-cell very early progenitors, as all other normal hematopoietic stem cells, were not destroyed and actually initiated a new wave of expansion, already 5 days after ACT. Consistent with our data, when B-cell depletion is obtained by anti-CD20 antibody therapy, the long half-life of serum antibodies maintains steady-state levels of circulating antibodies, and infection-related problems occur quite rarely in the clinic.[39]

To address the question about human tumor susceptibility to anti-TERT ACT, CD8$^+$ T cells specific for hTERT were obtained in HLA-A2 transgenic mice after active immunization with DNA coding for hTERT. T cells capable of lysing human tumors, including a Burkitt lymphoma, were obtained with hTERT$_{865-872}$ peptide but not with other TERT-derived peptides. A crucial requirement for an effective cancer therapy concerns cancer stem cell resistance to treatment. Cancer stem cells have the greatest proliferative capacity and are, potentially, the favorite target for anti-TERT immune attack. Data with HLA-A2–restricted CTLs suggest that TERT-based ACT has certainly the potential to recognize and destroy the pool of cancer cells endowed with stemness, eliminating cells that might survive other forms of therapy, such as chemotherapy and radiotherapy.

Data presented here are supportive of a broad clinical application of TERT-directed ACT, on the basis of the effectiveness on many tumor histotypes and the induction of a temporary autoimmune depletion of B cells as main side effect. Therapeutic activity against the human Burkitt lymphoma DG-75 also opens to additional developments. These findings, in fact, suggest that the selective effect on B cells might be further explored either in mice that develop autochthonous lymphomas or in human B-cell lymphomas grown in immunodeficient mice.

Authorship

Contribution: V.B. designed research; S.U., M.I., C.M., T.P., F.C., R.D.P, and B.C. performed research; L.R.V. provided critical reagents; E.S., R.D.P., E.P., P.Z., and P.M. analyzed data; and S.U., E.S., and V.B. wrote the paper.

Conflict-of-interest disclosure: E.S., C.M., F.C., and B.C. are employees of IRBM, Merck Research Laboratories, Italy. The remaining authors declare no competing financial interests.

Correspondence: Vincenzo Bronte, MD, Istituto Oncologico Veneto (IOV), Via Gattamelata 64, 35128 Padova, Italy; e-mail: enzo.bronte@unipd.it.

References

1. Mitchison NA. Studies on the immunological response to foreign tumor transplants in the mouse. I. The role of lymph node cells in conferring immunity by adoptive transfer. *J Exp Med.* 1955; 102(2):157-177.

2. Rosenberg SA, Packard BS, Aebersold PM, et al. Use of tumor-infiltrating lymphocytes and interleukin-2 in the immunotherapy of patients with metastatic melanoma. A preliminary report. *N Engl J Med.* 1988;319(25):1676-1680.

3. Dudley ME, Wunderlich JR, Robbins PF, et al. Cancer regression and autoimmunity in patients after clonal repopulation with antitumor lymphocytes. *Science.* 2002;298(5594):850-854.

4. Dudley ME, Wunderlich JR, Yang JC, et al. Adoptive cell transfer therapy following non-myeloablative but lymphodepleting chemotherapy for the treatment of patients with refractory metastatic melanoma. *J Clin Oncol.* 2005;23(10):2346-2357.

5. Harley CB. Telomerase and cancer therapeutics. *Nat Rev Cancer.* 2008;8(3):167-179.

6. Su Z, Dannull J, Yang BK, et al. Telomerase mRNA-transfected dendritic cells stimulate antigen-specific CD8$^+$ and CD4$^+$ T-cell responses in patients with metastatic prostate cancer. *J Immunol.* 2005; 174(6):3798-3807.

7. Domchek SM, Recio A, Mick R, et al. Telomerase-specific T-cell immunity in breast cancer: effect of vaccination on tumor immunosurveillance. *Cancer Res.* 2007;67(21):10546-10555.

8. Vonderheide RH. Universal tumor antigens for cancer vaccination: targeting telomerase for immunoprevention. *Discov Med.* 2007;7(39):103-108.

9. Chen DY, Vance BA, Thompson LB, Domchek SM, Vonderheide RH. Differential lysis of tumors by polyclonal T-cell lines and T-cell clones specific for hTERT. *Cancer Biol Ther.* 2007;6(12): 1991-1996.

10. Greenberg NM, DeMayo F, Finegold MJ, et al. Prostate cancer in a transgenic mouse. *Proc Natl Acad Sci U S A.* 1995;92(8):3439-3443.

11. Ricci-Vitiani L, Lombardi DG, Pilozzi E, et al. Identification and expansion of human colon-cancer–initiating cells. *Nature.* 2007;445(7123): 111-115.

12. Montgomery DL, Shiver JW, Leander KR, et al. Heterologous and homologous protection against influenza A by DNA vaccination: optimization of DNA vectors. *DNA Cell Biol.* 1993;12(9):777-783.

13. Arai K, Masutomi K, Khurts S, Kaneko S, Kobayashi K, Murakami S. Two independent regions of human telomerase reverse transcriptase are important for its oligomerization and telomerase activity. *J Biol Chem.* 2002;277(10):8538-8544.

14. Mennuni C, Ugel S, Mori F, et al. Preventive vaccination with telomerase controls tumor growth in genetically engineered and carcinogen-induced

mouse models of cancer. *Cancer Res.* 2008; 68(23):9865-9874.

15. Kern F, Faulhaber N, Frommel C, et al. Analysis of CD8 T-cell reactivity to cytomegalovirus using protein-spanning pools of overlapping pentade-capeptides. *Eur J Immunol.* 2000;30(6):1676-1682.

16. Draenert R, Altfeld M, Brander C, et al. Comparison of overlapping peptide sets for detection of antiviral CD8 and CD4 T-cell responses. *J Immunol Methods.* 2003;275(1-2):19-29.

17. De Palma R, Marigo I, Del Galdo F, et al. Therapeutic effectiveness of recombinant cancer vaccines is associated with a prevalent T-cell receptor alpha usage by melanoma-specific CD8+ T lymphocytes. *Cancer Res.* 2004;64(21):8068-8076.

18. Wu Y, Tworkoski K, Michaud M, Madri JA. Bone marrow monocyte PECAM-1 deficiency elicits increased osteoclastogenesis resulting in trabecular bone loss. *J Immunol.* 2009;182(5):2672-2679.

19. Osati-Ashtiani F, King LE, Fraker PJ. Variance in the resistance of murine early bone marrow B cells to a deficiency in zinc. *Immunology.* 1998; 94(1):94-100.

20. Shappell SB, Thomas GV, Roberts RL, et al. Prostate pathology of genetically engineered mice: definitions and classification. The consensus report from the Bar Harbor meeting of the Mouse Models of Human Cancer Consortium Prostate Pathology Committee. *Cancer Res.* 2004;64(6):2270-2305.

21. Raina K, Blouin MJ, Singh RP, et al. Dietary feeding of silibinin inhibits prostate tumor growth and progression in transgenic adenocarcinoma of the mouse prostate model. *Cancer Res.* 2007;67(22): 11083-11091.

22. Gattinoni L, Powell DJ Jr, Rosenberg SA, Restifo

NP. Adoptive immunotherapy for cancer: building on success. *Nat Rev Immunol.* 2006;6(5):383-393.

23. Overwijk WW, Theoret MR, Finkelstein SE, et al. Tumor regression and autoimmunity after reversal of a functionally tolerant state of self-reactive CD8+ T cells. *J Exp Med.* 2003;198(4):569-580.

24. Gattinoni L, Finkelstein SE, Klebanoff CA, et al. Removal of homeostatic cytokine sinks by lymphodepletion enhances the efficacy of adoptively transferred tumor-specific CD8+ T cells. *J Exp Med.* 2005;202(7):907-912.

25. Vonderheide RH, Hahn WC, Schultze JL, Nadler LM. The telomerase catalytic subunit is a widely expressed tumor-associated antigen recognized by cytotoxic T lymphocytes. *Immunity.* 1999;10(6): 673-679.

26. Cappelletti M, Zampaglione I, Rizzuto G, Ciliberto G, La Monica N, Fattori E. Gene electro-transfer improves transduction by modifying the fate of intramuscular DNA. *J Gene Med.* 2003;5(4):324-332.

27. Minev B, Hipp J, Firat H, Schmidt JD, Langlade-Demoyen P, Zanetti M. Cytotoxic T-cell immunity against telomerase reverse transcriptase in humans. *Proc Natl Acad Sci U S A.* 2000;97(9): 4796-4801.

28. Thorn M, Wang M, Kloverpris H, et al. Identification of a new hTERT-derived HLA-A*0201 restricted, naturally processed CTL epitope. *Cancer Immunol Immunother.* 2007;56(11):1755-1763.

29. Rosenberg SA, Restifo NP, Yang JC, Morgan RA, Dudley ME. Adoptive cell transfer: a clinical path to effective cancer immunotherapy. *Nat Rev Cancer.* 2008;8(4):299-308.

30. Terrin L, Rampazzo E, Pucciarelli S, et al. Relationship between tumor and plasma levels of hTERT mRNA in patients with colorectal cancer: implications for monitoring of neoplastic disease. *Clin Cancer Res.* 2008;14(22):7444-7451.

31. Grochola LF, Greither T, Taubert HW, et al. Prognostic relevance of hTERT mRNA expression in ductal adenocarcinoma of the pancreas. *Neoplasia.* 2008;10(9):973-976.

32. Vonderheide RH. Prospects and challenges of building a cancer vaccine targeting telomerase. *Biochimie.* 2008;90(1):173-180.

33. Bono AV, Montironi R, Pannellini T, et al. Effects of castration on the development of prostate adenocarcinoma from its precursor HGPIN and on the occurrence of androgen-independent, poorly differentiated carcinoma in TRAMP mice. *Prostate Cancer Prostatic Dis.* 2008;11(4):377-383.

34. Damber JE, Aus G. Prostate cancer. *Lancet.* 2008;371(9625):1710-1721.

35. Palmer DC, Chan CC, Gattinoni L, et al. Effective tumor treatment targeting a melanoma/melanocyte-associated antigen triggers severe ocular autoimmunity. *Proc Natl Acad Sci U S A.* 2008;105(23): 8061-8066.

36. Tsuboi I, Hirabayashi Y, Harada T, et al. Predominant regeneration of B-cell lineage, instead of myeloid lineage, of the bone marrow after 1 Gy whole-body irradiation in mice: role of differential cytokine expression between B-cell stimulation by IL10, Flt3 ligand and IL7 and myeloid suppression by GM-CSF and SCF. *Radiat Res.* 2008;170(1): 15-22.

37. Cabatingan MS, Schmidt MR, Sen R, Woodland RT. Naive B lymphocytes undergo homeostatic proliferation in response to B-cell deficit. *J Immunol.* 2002;169(12):6795-6805.

38. van Zelm MC, van der Burg M, van Dongen JJ. Homeostatic and maturation-associated proliferation in the peripheral B-cell compartment. *Cell Cycle.* 2007;6(23):2890-2895.

39. Edwards JC, Szczepanski L, Szechinski J, et al. Efficacy of B-cell–targeted therapy with rituximab in patients with rheumatoid arthritis. *N Engl J Med.* 2004;350(25):2572-2581.